

NUMERICAL SIMULATION OF VORTEX RING STATE PHENOMENON FOR THE MI2 TYPE HELICOPTER TAIL ROTOR

Wiesław Zalewski

Institute of Aviation
Krakowska Avenue 110/114, 02-256 Warsaw, Poland
tel.: +48 22 8460011, fax: +48 22 8464432
e-mail: wieslaw.zalewski@ilot.edu.pl

Abstract

The paper presents computational simulations of loss of helicopter tail rotor effectiveness (LTE) effect caused by rotor vortex ring state (VRS) phenomenon. The phenomenon is critical for safety of helicopter operations and it was an important factor in some military and civil helicopters serious accidents. Analysis was conducted on the example of the tail rotor of Mi2 and PZL Kania single main rotor medium helicopters, which are still in wide use in some parts of the world. That kind of dual blades tail rotor was designed with symmetrical NACA0012 airfoil. Full three-dimensional analysis of the flow around real geometry of the rotor blades was conducted by application of commercial solver Ansys Fluent.

The simulation was made by resolving Unsteady Reynolds Averaged Navier Stokes equations by finite volume method with use of Moving Mesh and Moving Reference Frame techniques. A hover turn over a spot was chosen as flight condition of helicopter, which could induce the LTE phenomenon. Thrust and power consumption were estimated during computations. Visualization of the flow field and pathlines of the flow were presented for chosen stages of vortex ring formulation around the rotor. The sensitivity of dual blades tail rotors, which are popular in light and medium type of helicopters to LTE phenomenon, was estimated.

Keywords: air transport, helicopters, tail rotor VRS

1. Introduction

Currently, the most typical layout of helicopters is the system with the single main rotor and the tail rotor (Fig. 1). Helicopters of this type are exposed to the occurrence of loss of the tail rotor effectiveness (LTE) phenomenon, which causes an unexpected decrease in the thrust generated by the tail rotor. As a result, it can lead to the loss of directional control of the helicopter and the entry into uncontrollable rotation around the vertical axis, what is called unanticipated yaw. One of the important elements of helicopter pilots training is the ability to avoid the flight conditions conducive to LTE and methods for rapid exit from a state of emergency in the early stage of its development. It is estimated that between 1996 and 2005 about 61 serious helicopter accidents were caused by LTE phenomenon [2, 10].

There are three basic aerodynamic conditions inducing LTE [2]:

- main rotor disc vortex interference with the tail rotor,
- weathercock stability (tailwinds presence),
- tail vortex ring state.

In this paper, the numerical analysis of the tail vortex ring state phenomenon was presented.

For the analysis, a tail rotor used in Mi2 [9] and PZL Kania helicopters was selected. That type of light helicopters is still in operation in several countries in the world. The tail rotor blades were designed on the basis of NACA0012 symmetrical airfoil. This airfoil is now being replaced by dedicated for helicopter applications; modern asymmetrical airfoils designed using advanced calculation and optimization methods [6-8].

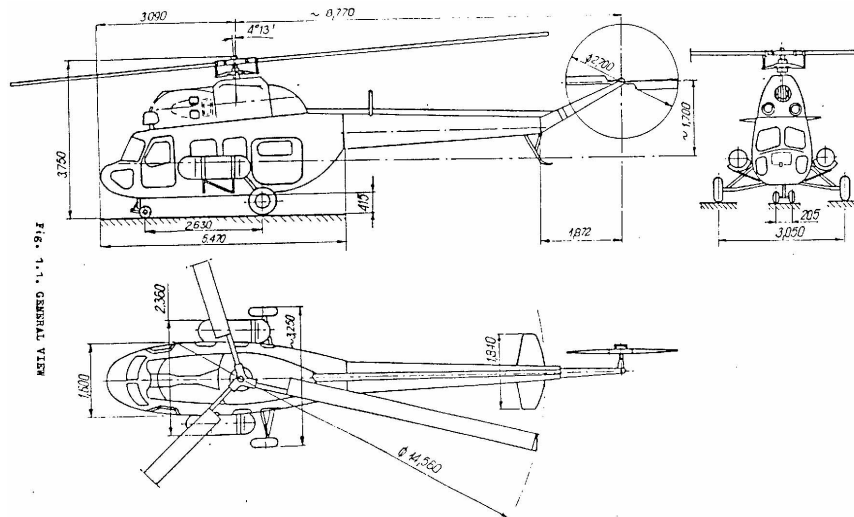


Fig. 1. Mil Mi 2 and PZL Kania helicopter [5]

2. Model

Due to the complexity of the phenomenon, in most of the papers about the LTE, simplified numerical models of working main and tail rotors are used. During these simulations an actuator disc model of fan is applied, which assumes that a rotor is replaced by a pressure jump-generating surface [1, 3]. In more advanced simulations, the virtual blade model (VBM) is preferred. It is based on the blade element theory and uses 2D aerodynamic characteristics of airfoils, which were used in cross-sections of the blades [4]. The big advantage of this type of modelling is simplicity, short time of calculations and the ability to take into account the presence of the helicopter structure (fuselage, tail boom) and the mutual influence of the helicopter tail rotor and main rotor. The most accurate results, however, provide a method of modelling the full geometry of the rotor blades based on solving averaged Navier-Stokes equations with finite volume method combined with Moving Mesh techniques in a transient state and Moving Reference Frame in transient or steady state conditions. That method was chosen to carry out the simulations presented in this paper.

Simulations were performed for the isolated tail rotor model with the use of Ansys Fluent commercial computational fluid dynamic solver. A high-quality mesh of a full 3D geometry of the tail rotor blades was prepared to analysis (Fig. 2). The moving part of the computational mesh was made as two cylinders containing the rotor blades. The part of the far flow field around cylinders was made as a mesh with tetrahedral elements. The interface type boundary condition was applied for sliding connection of cylinders and far flow field meshes (Fig. 3). Simulations were performed for static and dynamic vortex ring formulation.

3. Results of simulation

3.1. Vortex ring state formulation in static conditions

In the first part of the simulation, a phenomenon of generating ring vortex state by the airflow directed opposite to the speed induced by the rotor was analysed. Such approach is typical for wind tunnel tests. Rotor blades were operated at constant pitch angle (15 deg) and constant rotational speed (1445 rpm). The external far field airflow velocity was increased from 0 to 30 m/s. The simulation was focused at determination of the velocity range of occurrence a ring vortex state phenomenon for rotor with constant blades pitch angle and a comparison with approximate analytical formulas used to determine that range [3].

The theoretical range of the vortex ring state phenomenon occurrence is assumed to be $0.5-1.5 V_i$, where V_i is a flow speed induced by the rotor. In the tested configuration of the rotor, the effects

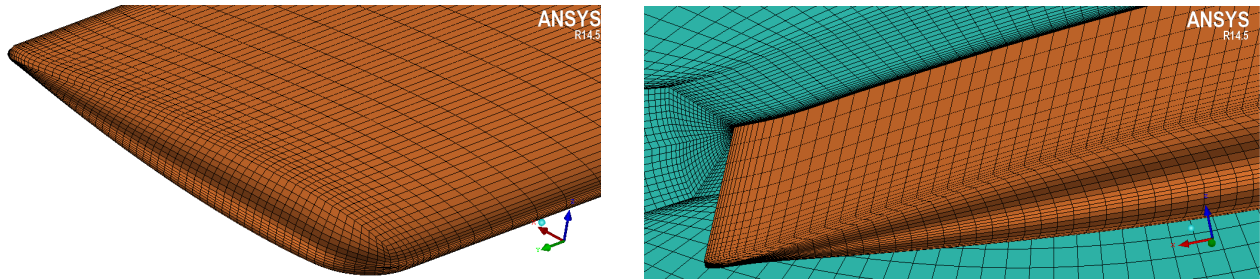


Fig. 2. High quality hexahedral mesh around a blade prepared in Ansys ICEM CFD software

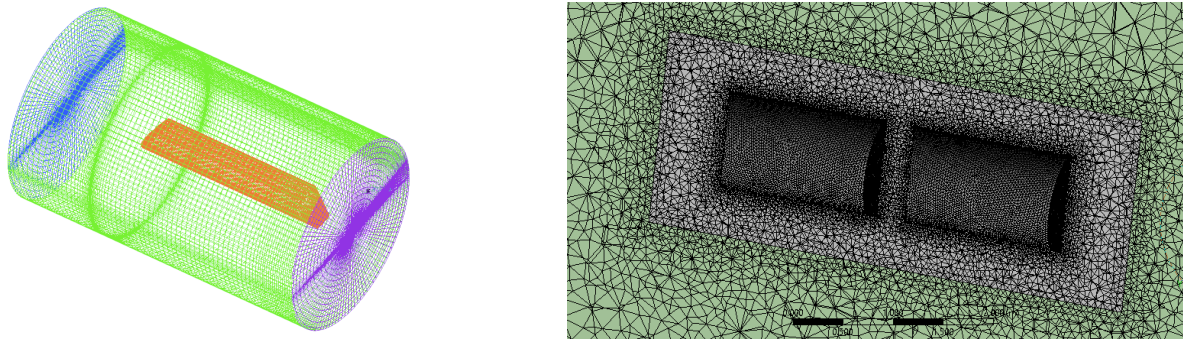


Fig. 3. The cylinder with a single blade and tetrahedral fluid mesh connected with the cylinders by sliding interfaces

of vortex ring state occurrence should appear in a range of external flow speed $v = 8.4\text{-}25.2$ m/s. The main effect of the vortex ring state condition is a drop of thrust value generated by the rotor.

During the calculation, the rotor thrust F_z was determined (Fig. 4) and pathline visualization of the flow field for the subsequent stages of formulation of vortex ring state was performed (Fig. 5). Steady state condition, Spalart-Allmaras turbulence model and compressible viscous flow were assumed.

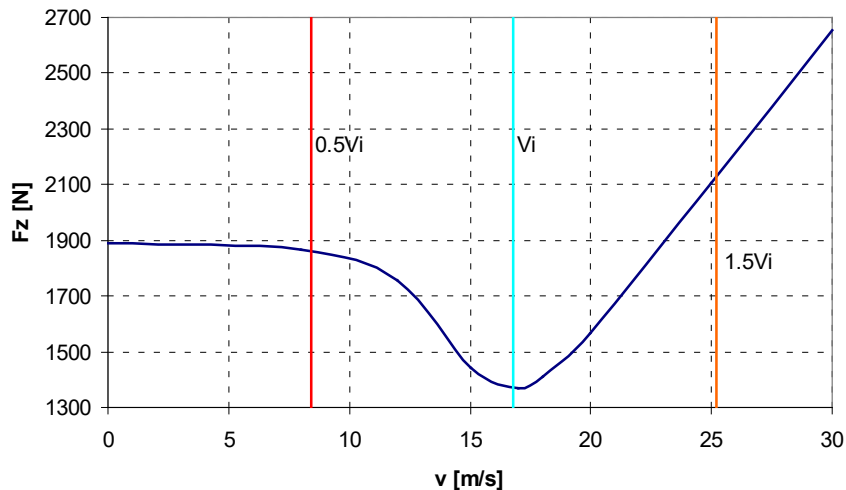


Fig. 4. Thrust variation for a single blade of the tail rotor with velocity of wind that opposes the tail rotor induced airflow

3.2. Vortex ring state formulation in dynamic conditions

As part of the performed numerical analyses, the phenomenon of vortex ring state creation around the tail rotor, in conditions similar to the real dynamic manoeuvre of the helicopter, was also studied. The hover turn over a spot was chosen as flight condition for helicopter, which could induce the LTE phenomenon. The hover turn was started by changing the pitch angle of rotor blades to the value of -5 deg. Once the helicopter fuselage angular speed of 1.63 rad/s was reached.

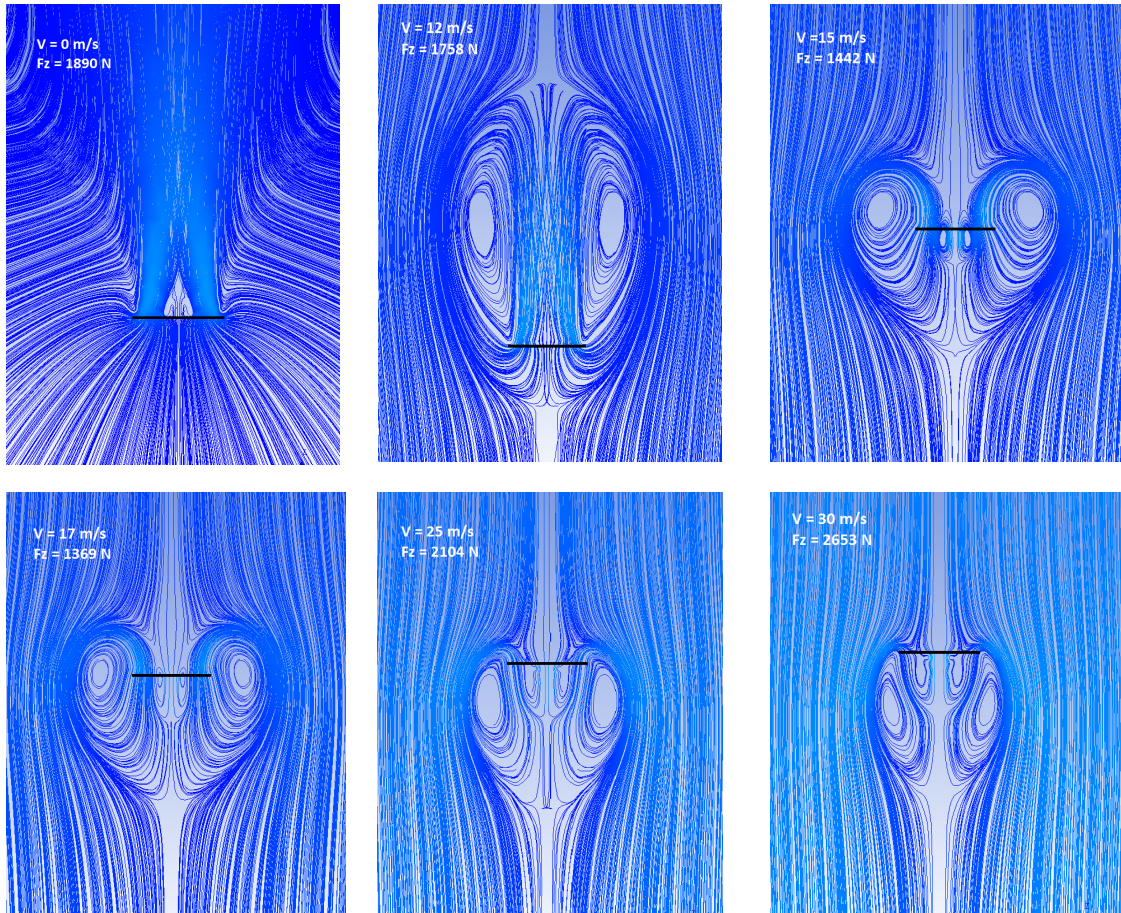


Fig. 5. Pathlines visualisation for subsequent stages of vortex ring state formulation (rotor marked as black line) in 3D steady simulation for different velocity of wind (0, 12, 15, 17, 25, 30 m/s) that opposes the tail rotor induced airflow

corresponding to an average velocity of airflow of about 14 m/s against the tail rotor, the rotation was countered by pilot through rapid changing the pitch of the tail rotor blades to 20 degrees (maximum deflection) at a rate of 50 degrees per second.

During the simulation, the variation of thrust F_z with time T for a single rotor blade was calculated (Fig. 6) and corresponding power consumption (Fig. 7).

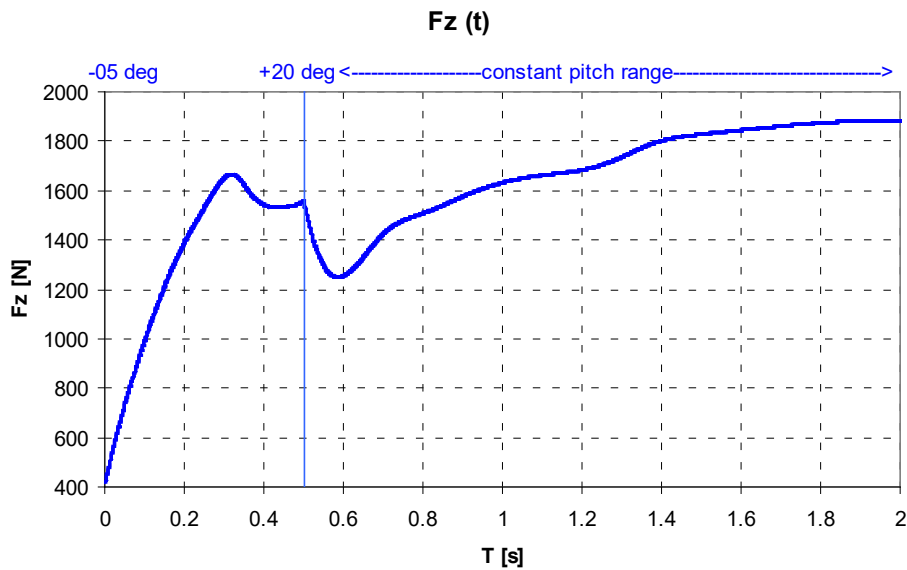


Fig. 6. Thrust (F_z) variation for a single blade of the tail rotor with the time (T) of the manoeuvre

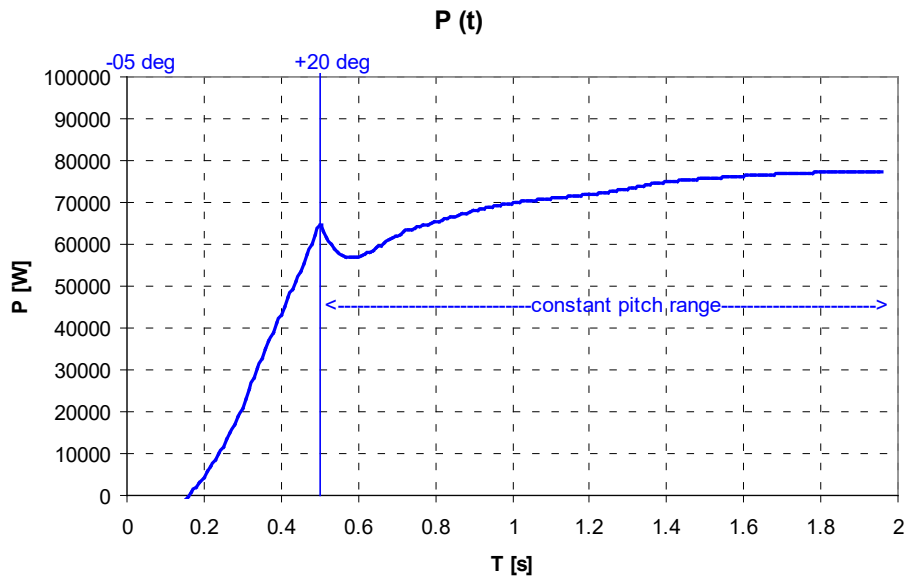


Fig. 7. Power (P) consumption for a single blade of the tail rotor with time (T) of the manoeuvre

The pathlines of the flow in the plane lying in the axis of the rotor and perpendicular to the plane of its rotation were presented in Fig. 8.

Calculations were performed as full 3D, unsteady simulation for isolated tail rotor (the impact of the fuselage and interference with the main rotor flow were not taken into account) with Spalart-Allmaras turbulence model and compressible viscous flow assumptions. Results for the first 2 seconds of manoeuvre were shown in the figures below.

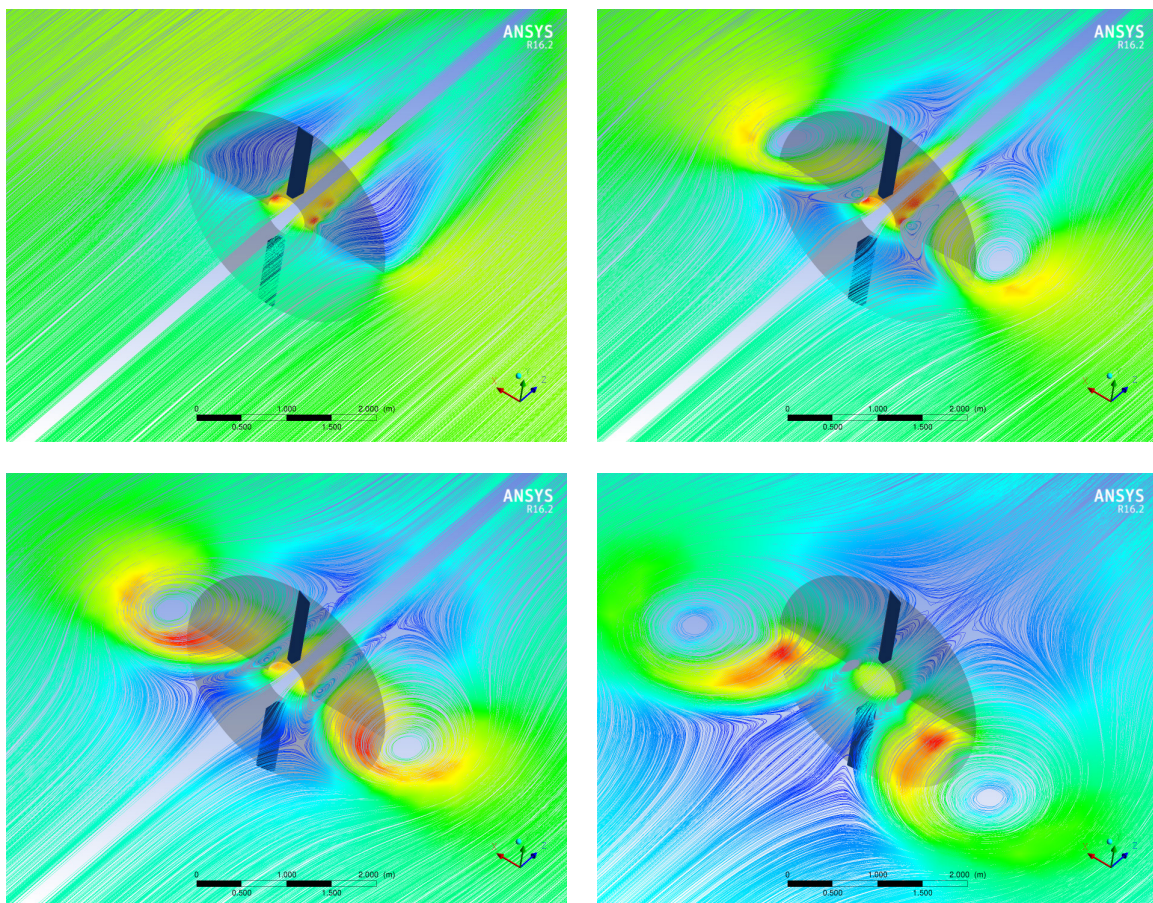


Fig. 8. Pathlines visualisation for subsequent stages of vortex ring state formulation in full 3D unsteady simulation

4. Conclusions

In conducted analysis, the decrease in the thrust of the tail rotor due to the vortex ring state phenomenon was in range from 26% to 34% of thrust of the tail rotor.

It is worth emphasizing that the biggest drop in thrust occurred in conditions similar to the conditions of real manoeuvre of a helicopter.

Computed range of the influence of the vortex ring state phenomenon is very close to what gives the theory.

The maximum impact of the vortex ring state phenomenon for decreasing thrust appears when the forward speed of the tail rotor (caused by hover turn of the helicopter) is equal in value and opposite to the flow speed induced by the rotor.

The largest loss of thrust occurs when the centre of the vortex ring is located in the extension of plane of blades rotation.

The tail rotors, which generate higher speed of inducted airflow, are less susceptible to the ring vortex state phenomenon.

References

- [1] Dziubiński, A., Stalewski, W., *Vortex ring state simulation using actuator disc*, Instytut Lotnictwa, Proceedings 21st European Conference on Modelling and Simulation, 2007.
- [2] Cuzieux, F., Basset, P.-M., Desoppe, A., *Modeling of loss of tail rotor effectiveness conducting to unanticipated yaw*, ICAS 2012, 28th International Congress of the Aeronautical Science, 2012.
- [3] Florczuk, W., *Analiza powstawania pierścienia wirowego wokół wirnika głównego na podstawie badań śmigłowca W-3 Sokół przy użyciu pakietu obliczeniowego FLUENT*, Prace Instytutu Lotnictwa, Nr 6 (201), Warszawa, 2009.
- [4] Grzegorzczak, K., *Modelowanie lotu śmigłowca w warunkach występowania pierścienia wirowego za pomocą virtual blade model*, Modelowanie Inżynierskie, Vol. 14, Nr 45, 2012.
- [5] <http://barrieaircraft.com/photo/pzl-swidnik-mil-mi2-kania-02.html>.
- [6] Kania, W., Stalewski, W., *Development of new generation main and tail rotors blade airfoils*, ICAS 2000 Congress, 2000.
- [7] Kania, W., Stalewski, W., Zwierchanowska, B., *Design of the modern family of helicopter airfoils*, Transactions of the Institute of Aviation, No. 191. Warsaw 2007.
- [8] Kania, W., Stalewski, W., Zwierchanowska, B., *Inverse and direct optimistaion of tail rotor airfoil using genetic algorithm*, Proceedings of the Forth International Seminar on RRDPAE'2000, Warszawa 2000.
- [9] Mil, M. L., *Helicopters, Calculation and design*, NASA, Washington, September 1967.
- [10] Prouty, R. W., *A Possible Tail Rotor Problem*, Vertiflight, January/February 2012.